SPANDIDOS PUBLICATIONS

MOLECULAR MEDICINE REPORTS 31: 19, 2025

4-Methoxydalbergione inhibits the tumorigenesis and metastasis of lung cancer through promoting ferroptosis via the DNMT1/system X_c^-/GPX4 pathway

JUN FAN*, HAORAN LIN*, JINHUA LUO and LIANG CHEN

Department of Thoracic Surgery, The First Affiliated Hospital of Nanjing Medical University, Nanjing, Jiangsu 210000, P.R. China

Received July 8, 2024; Accepted September 10, 2024

DOI: 10.3892/mmr.2024.13384

Abstract. Lung cancer is responsible for the highest number of tumor-related deaths worldwide. A flavonoid extracted from the heartwood of *Dalbergia sissoo* Roxb., 4-methoxydalbergione (4-MD), exhibits potent anticancer activity in multiple malignancies; however, the potential anticancer activity of 4-MD in lung cancer has not yet been elucidated. In the present study, A549 cells were treated with increasing concentrations of 4-MD, and cell viability was assessed using a Cell Counting Kit-8 assay. In addition, colony formation, 5-ethynyl-2'-deoxyuridine, wound healing and Transwell assays were conducted to evaluate cell proliferation, migration and invasion, respectively. Cell morphology was observed using transmission electron microscopy, and ferroptosis was determined using thiobarbituric acid reactive substance, lipid reactive oxygen species (ROS) and iron assays. Moreover, molecular docking was used to verify the potential interaction between 4-MD and DNA methyltransferase 1 (DNMT1). Tumor-bearing mice were established and treated with 10 or 30 mg/kg 4-MD, and tumor volume and weight were recorded. Immunohistochemistry and Prussian blue staining were conducted to examine Ki-67 expression and iron deposition in tumor tissues, and protein expression was further explored using western blot analysis. The results of the present study revealed that 4-MD significantly inhibited cell proliferation, migration, invasion and epithelial-mesenchymal transition in a concentration-dependent manner. Notably, 4-MD induced ferroptosis via increased lipid peroxidation, lipid ROS and Fe^{2+} levels. In addition, it was revealed that 4-MD can directly bind to DNMT1 to inhibit expression, and inhibit solute carrier family 7 member 11 (SLC7A11; also known as cystine-glutamate antiporter) and glutathione peroxidase 4 expression. Following DNMT1 overexpression, the observed antitumor activity and ferroptosis-promoting effects of 4-MD were partially reversed. Furthermore, 4-MD significantly inhibited tumor growth *in vivo*, and reduced tumor volume and weight. In addition, Ki-67 expression was reduced while iron deposition was increased in the tumor tissues of mice following treatment with 4-MD. In conclusion, 4-MD may exhibit anticancer activity through the promotion of DNMT1-mediated cell ferroptosis. Thus, 4-MD may have potential as a novel therapeutic agent in the treatment of lung cancer.

Correspondence to: Dr Liang Chen, Department of Thoracic Surgery, The First Affiliated Hospital of Nanjing Medical University, 300 Guangzhou Road, Gulou, Nanjing, Jiangsu 210000, P.R. China
E-mail: chenliangcl_2023@163.com

*Contributed equally

Key words: lung cancer, 4-methoxydalbergione, DNA methyltransferase 1, ferroptosis

Introduction

Lung cancer is the most commonly diagnosed type of cancer and the leading cause of cancer-related deaths worldwide. At present, the number of cases of non-small cell lung cancer, the main pathological subtype of lung cancer, are increasing annually (1). Despite notable advancements in chemotherapy, radiotherapy and molecular targeted therapy, the 5-year survival rate of patients with lung cancer remains at <20%, and patients exhibit high mortality rates (2). Notably, metastasis is a key cause for treatment failure and poor survival rates of patients with lung cancer, leading to 90% of lung cancer-related deaths (3,4). Thus, the development of novel, effective and reliable therapeutic drugs is required for the clinical treatment of lung cancer.

Research has focused on the potent anticancer activity of traditional herbal medicines (5). 4-Methoxydalbergione (4-MD) is a flavonoid extracted from the heartwood of *Dalbergia sissoo* Roxb., which has anti-inflammatory and cytoprotective properties (6,7). The results of previous studies revealed that 4-MD exhibits anticancer activity in numerous malignancies, including bladder cancer, liver cancer, esophageal carcinoma, astroglioma and osteosarcoma; therefore, 4-MD may have potential as a therapeutic agent against various types of cancer (8-12). However, the effects of 4-MD on lung cancer have yet to be fully elucidated.

The induction of tumor cell death is an approach for cancer therapy. Ferroptosis, an iron-dependent form of regulated cell death, is characterized by the accumulation of lipid reactive oxygen species (ROS), altered mitochondrial morphology and depletion of the endogenous antioxidant glutathione (GSH). Moreover, ferroptosis is driven by iron-dependent

lipid peroxidation (13,14), and this process is involved in the regulation of cancer invasion, angiogenesis and metastasis. The results of a previous study revealed that the induction of ferroptosis may exhibit potential as a strategy for the inhibition of cancer cells and the mitigation of cancer metastasis (15).

The present study aimed to characterize the anticancer effect of 4-MD on lung cancer *in vivo* and *in vitro*, and to elucidate the molecular mechanism of 4-MD against lung cancer. These findings suggested 4-MD as a promising therapeutic drug for lung cancer treatment.

Materials and methods

Cell culture and treatment. The lung cancer cell line A549 was obtained from Procell Life Science & Technology Co., Ltd., and was cultured in F12K medium (Gibco; Thermo Fisher Scientific, Inc.) supplemented with 10% fetal bovine serum (FBS; Gibco; Thermo Fisher Scientific, Inc.) and 1% penicillin/streptomycin in a humidified incubator with 5% CO_2 at 37˚C. Cells were treated with 4-MD (purity, 98%; Shanghai Yuanye Biotechnology Co., Ltd.) dissolved in dimethyl sulfoxide (DMSO) at an initial concentration of 50 mM. A549 cells were treated with increasing concentrations of 4-MD (3.125, 6.25, 12.5, 25, 50, 100, 200, 400 and 800 μM) for 24 h at 37˚C. Additionally, A549 cells with or without Oe-DNMT1 transfection were treated with 50 μM 4-MD for 24 h at 37˚C.

Cell viability assay. A total of $1x10^3$ cells were seeded into 96-well plates and cultured at 37˚C in a humidified incubator with 5% CO_2. At 24, 48 and 72 h, 10 μl CCK-8 solution (Shanghai Yeasen Biotechnology Co., Ltd.) was added to each well, and the cells were incubated for a further 3 h at 37˚C. The absorbance of each well was measured at 450 nm using a microplate reader (Omega Bio-Tek, Inc.).

Colony formation assay. A549 cells were seeded into plates (1,000 cells/well) and were cultivated in medium containing 10% FBS for 2 weeks. When cell colonies were visible to the naked eye, A549 cells were fixed with 4% paraformaldehyde for 5 min and stained with 0.1% crystal violet 20 min, both at room temperature. The colonies (>50 cells) were counted using a light microscope (Olympus Corporation) and ImageJ 1.8.0 software (version 1.8.0; National Institutes of Health).

5-Ethynyl-2'-deoxyuridine (EDU) analysis. A549 cells ($5x10^4$ cells/well) were seeded into 96-well plates and cultured at 37˚C for 24 h. In total, 100 μl diluted EDU solution (Thermo Fisher Scientific, Inc.) was added to each well, and the cells were cultured for a further 2 h at 37˚C. Subsequently, the cells were fixed with 4% paraformaldehyde for 30 min and permeabilized with 5% Triton X-100 for 15 min at room temperature. Cell nuclei were stained with DAPI staining solution (Beyotime Institute of Biotechnology) at 37˚C for 30 min. EDU-positive cells were observed under a fluorescence microscope (Olympus Corporation).

Wound healing assay. Once A549 cells reached 90% confluence, a scratch was created on the cell monolayer in a 6-well plate using a 200-μl pipette tip. The cells were then washed with PBS and were cultured in serum-free medium at 37˚C for 24 h. Images of the wound were captured at 0 and 24 h using a light microscope (Olympus Corporation), and wound healing was recorded to assess cell migration.

Transwell invasion assay. A549 cells ($5x10^5$ cells/well) were resuspended in serum-free medium and seeded into the upper chamber of a 24-well plate (Transwell insert; 8 μm pores; Corning, Inc.). To assess cell invasion, the membranes were precoated with Matrigel overnight at 37˚C. The lower chamber was filled with complete medium supplemented with 10% FBS as a chemoattractant. Following incubation for 24 h at 37˚C, invasive cells were fixed with 100% methanol for 10 min at 37˚C and stained with crystal violet for 15 min at 37˚C. Subsequently, images of the cells were captured using a light microscope (Olympus Corporation) and they were counted.

Reverse transcription-quantitative PCR (RT-qPCR). Total RNA was extracted from $5x10^5$ A549 cells using TRIzol® reagent (Invitrogen; Thermo Fisher Scientific, Inc.) and the PrimeScript RT reagent kit (Takara Bio, Inc.) was used to generate cDNA, according to the manufacturers' recommendations. The ABI 7500 Real-Time PCR System (Applied Biosystems; Thermo Fisher Scientific, Inc.) was employed to conduct qPCR with the SYBR-Green PCR Master Mix (Takara Bio, Inc.) according to the manufacturer's protocol. The following thermocycling conditions were used: Initial denaturation at 95˚C for 10 min; followed by 35 cycles of denaturation at 95˚C for 15 sec, annealing at 60˚C for 1 min and extension of 10 min at 65˚C. The relative mRNA expression levels were computed using the $2^{-\Delta\Delta Cq}$ method (16). GAPDH was used as the housekeeping control. The following primer sequences were used for qPCR: DNA methyltransferase 1 (DNMT1), forward 5'-TATCCGAGGAGGGCTACCTG-3', reverse, 5'-ATGAGCACCGTTCTCCAAGG-3'; GAPDH, forward 5'-AATGGGCAGCCGTTAGGAAA-3' and reverse 5'-GCGCCCAATACGACCAAATC-3'.

Western blot analysis. Total protein was extracted from A549 cells or mouse tissues using radioimmunoprecipitation assay lysis buffer (Beyotime Institute of Biotechnology). Total protein concentration was quantified using a bicinchoninic acid assay protein assay kit (Beyotime Institute of Biotechnology), and 30 μg/lane was then separated by sodium dodecyl-sulfate polyacrylamide gel electrophoresis on a 12% gel. Separated proteins were subsequently transferred to polyvinylidene fluoride membranes (MilliporeSigma) and blocked with non-fat milk at room temperature for 2 h. The membranes were then incubated with the following primary antibodies: Anti-E-cadherin (cat. no. 3195T; 1:1,000; Cell Signaling Technology, Inc.), anti-N-cadherin (cat. no. 22018-1-AP; 1:5,000; Proteintech Group, Inc.), anti-Vimentin (cat. no. ab92547; 1:1,000; Abcam), anti-DNMT1 (cat. no. ab188453; 1:1,000; Abcam), anti-solute carrier family 7 member 11 [SLC7A11; also known as cystine-glutamate antiporter; cat. no. ab307601; 1:1,000; Abcam), anti-GSH peroxidase 4 (GPX4; cat. no. ab125066; 1:1,000; Abcam), anti-acyl-CoA synthetase long-chain family 4 (ACSL4; cat. no. ab155282; 1:10,000; Abcam) and anti-GAPDH (cat. no. ab9485; 1:2,500; Abcam) at 4˚C overnight, followed by incubation with a horseradish peroxidase-conjugated goat anti-rabbit secondary antibody (cat. no. ab6721; 1:3,000;

Abcam) at room temperature for 2 h. Protein bands were visualized using an enhanced chemiluminescence kit (Beyotime Institute of Biotechnology) and were semi-quantified using ImageJ software (version 1.8.0).

Transmission electron microscopy. A549 cells were fixed with 2.5% glutaraldehyde for 5 min at 37˚C. Following centrifugation (1,000 x g) at room temperature for 10 min, the cells were fixed with 1% osmic acid for 2 h at room temperature. Cells were washed with phosphate buffer, dehydrated using alcohol and acetone, embedded with epoxy resin at room temperature for 2 h and sectioned (70-80 nm) using an ultramicrotome. The sections were stained with uranium-lead double staining (2% uranium acetate and 2.6% lead citrate) for 15 min at room temperature. Cells were then observed under a transmission electron microscope (JEM-2000EX; JEOL, Ltd.).

Measurements of lipid peroxidation and iron levels. Lipid peroxidation was assessed using thiobarbituric acid reactive substance (TBARS) and lipid ROS assays. For the TBARS assay (cat. no. C10445; Thermo Fisher Scientific, Inc.), $1x10^6$ cells were incubated with 7.5% trichloroacetic acid and 0.02% butylated hydroxyanisole for 15 min at room temperature. Following centrifugation (1,000 x g) at room temperature for 10 min, the supernatants were harvested, incubated with trichloroacetic acid and boiled for 10 min. After cooling, the absorbance was measured at 532 nm using a microplate reader (Omega Bio-Tek, Inc.).

To determine the levels of lipid peroxidation, $1x10^6$ cells were stained with 10 μM BODIPY (581/591) C11 (Invitrogen; Thermo Fisher Scientific, Inc.) at 37˚C for 30 min in the dark. Fluorescent signals were detected at 484/510 and 581/610 nm using a laser scanning confocal microscope (Olympus Corporation) to determine the levels of lipid ROS.

To determine the levels of Fe^{2+}, $5 x 10^4$ cells were stained with 1 μM FerroOrange (Fe^{2+} indicator; Shanghai Maokang Bio) at 37˚C for 30 min in the dark. Fluorescent signals were detected at 532/572 nm using a fluorescence microscope (Olympus Corporation).

Molecular docking. The target gene of 4-MD was predicted by TargetNet database (http://targetnet.scbdd.com/). The crystal structure of DNMT1 was acquired from Protein Data Bank (code, 4WXX; https://www.rcsb.org/). The 3-dimensional structure of 4-MD was obtained from PubChem Database (https://pubchem.ncbi.nlm.nih.gov/). Molecular docking was used to predict the optimal binding site of 4-MD for binding to DNMT1 (AutoDock 4.2, https://autodock.scripps.edu/). The optimal binding mode between 4-MD and DNMT1 was determined under the minimum binding free energy conformation (-5.9 kcal/mol) and visualized using PyMol (version, 1.8.2.0; DeLano Scientific, LLC).

Cell transfection. The human full-length DNMT1 was cloned into the pcDNA3.1 vector (Shanghai GenePharma Co., Ltd.) to generate the DNMT1-overexpression (Oe) vector (Oe-DNMT1). The empty pcDNA3.1 vector was used as the negative control (Oe-NC). A549 cells were seeded into 6-well plates and cultured at 37˚C in a humidified incubator with 5% CO_2. When cells reached 60-70% confluence, they were transfected with 50 ng/ml Oe-DNMT1 or Oe-NC using Lipofectamine® 3000 reagent (Invitrogen; Thermo Fisher Scientific, Inc.) at room temperature for 48 h according to the manufacturer's instructions. At 48 h post-transfection, cells were harvested for subsequent experiments.

Xenograft experiments. In total, 15 male BALB/c-nu mice (age, 4-6 weeks; weight, 18-20 g) were purchased from Shanghai SLAC Laboratory Animal Co., Ltd., and were housed in a standard environment (temp, 20-23˚C; humidity, 55±5%; 12-h light/dark cycle) with free access to water and food. All animal experiments were approved by the Animal Ethics Committee of The First Affiliated Hospital of Nanjing Medical University (approval no. IACUC-230814; Nanjing, China) and were carried out in accordance with the ARRIVE guidelines (17). Animals were divided into three groups (n=5 per group): Control group, 4-MD 10 mg/kg group and 4-MD 30 mg/kg group. In total, $4x10^6$ A549 cells were subcutaneously injected into the right flank of each mouse. After 7 days, A549 cell-inoculated mice were intraperitoneally injected with 4-MD (10 or 30 mg/kg in PBS and 0.01% DMSO) once every 3 days for 3 weeks. Control mice were injected with the same volume of solvent (PBS and 0.01% DMSO). Tumor size was measured every 3 days with a caliper, and tumor volume was calculated using the following equation: Length x $width^2/2$. Mice were sacrificed 28 days after cell injection with an intraperitoneal injection of 200 mg/kg sodium pentobarbital. Death was confirmed following observations of respiration, the heartbeat and pupils. Subsequently, tumors were excised and weighed. The health and behavior of the animals were monitored every day. A maximum tumor diameter of 20 mm, as well as tumor ulceration, infection or necrosis were considered the humane endpoints (18).

Immunohistochemistry (IHC) and Prussian blue staining. Lung tissues were harvested, fixed with 4% paraformaldehyde at 4˚C for 24 h, embedded in paraffin and cut into 4-μm sections. Following deparaffinization and rehydration in a descending series of ethanol, antigen retrieval was carried out using 0.1% sodium citrate buffer at 95˚C for 20 min, and sections were incubated with 3% hydrogen peroxide to block endogenous peroxidase activity and treated with 0.3% Triton X-100 to increases the permeability for 30 min at 37˚C. For Prussian blue staining, the sections were immersed in 1% potassium ferricyanide for 1 h at room temperature. For IHC staining, after blocking the sections with 10% goat serum (Beijing Solarbio Science & Technology Co., Ltd.) for 1 h at 37˚C, the sections were incubated with anti-DNMT1 (cat. no. ab188453; 1:100; Abcam) and anti-Ki-67 (cat. no. ab16667; 1:200; Abcam) antibody at 4˚C overnight, followed by incubation with a HRP-conjugated goat anti-rabbit secondary antibody (cat. no. ab6721; 1:1,000; Abcam) at 37˚C for 30 min. Sections were visualized using DAB, counterstained with hematoxylin for 2 min at room temperature, mounted in neutral gum and observed under an optical microscope (Olympus Corporation).

Statistical analysis. All data are presented as the mean ± standard deviation and all experiments were repeated at least three times. Statistical analysis was conducted using GraphPad Prism 8 (GraphPad Software; Dotmatics), and comparisons between groups were determined using one-way or two-way

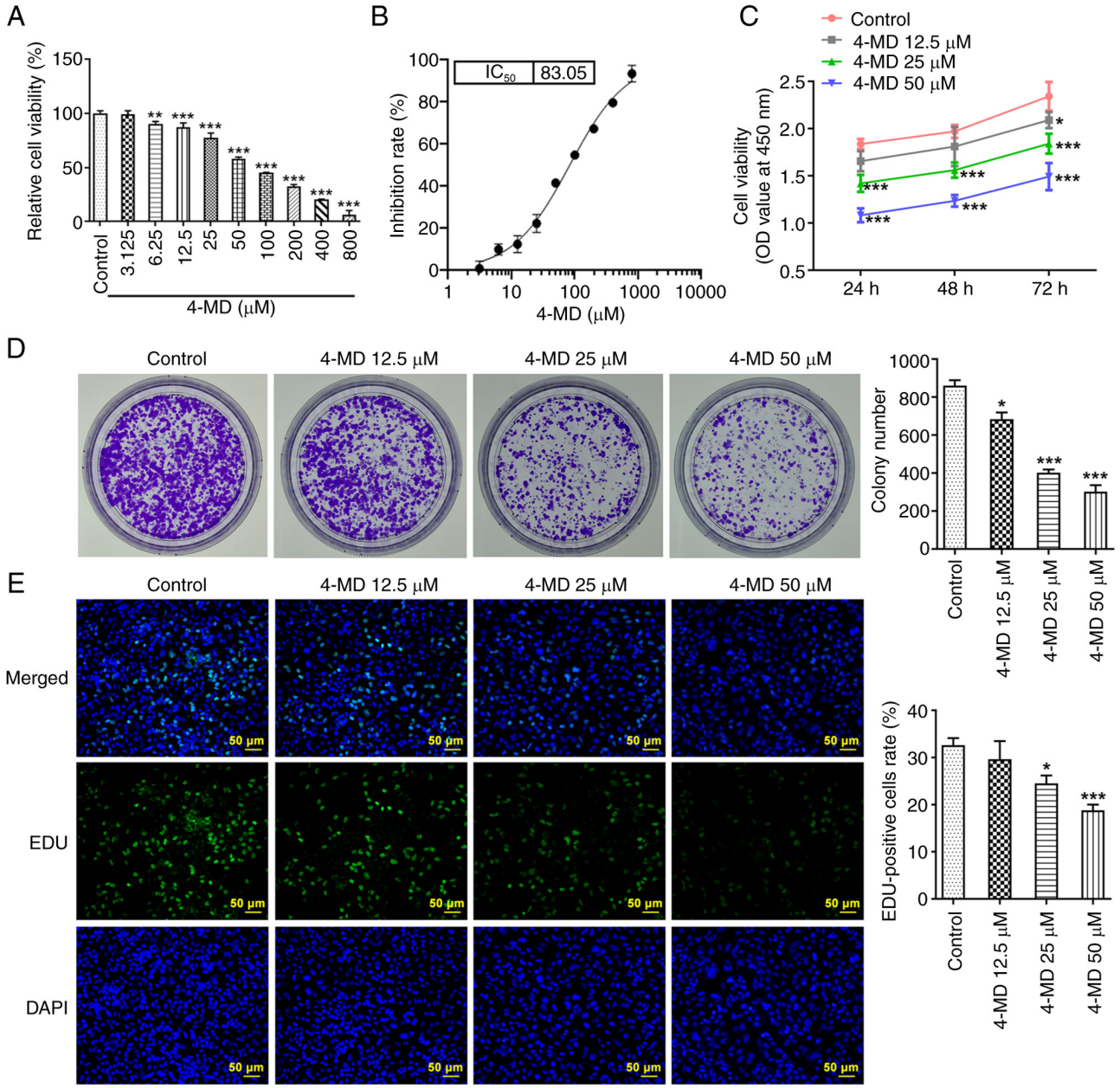

Figure 1. 4-MD suppresses the proliferation of A549 cells. (A) A549 cells were treated with increasing concentrations of 4-MD for 24 h, and cell viability was detected. (B) IC_{50} values were calculated. (C) A549 cells were treated with 4-MD (12.5, 25 and 50 μM) for 24, 48 and 72 h, and the absorbance was measured at 450 nm. (D) Colony formation assay was performed to examine the effect of 4-MD on A549 cell proliferation. (E) An EDU staining assay was performed to assess cell proliferation. *P<0.05, **P<0.01 and ***P<0.001 vs. Control. 4-MD, 4-methoxydalbergione; EDU, 5-ethynyl-2'-deoxyuridine.

analysis of variance followed by Tukey's post hoc test. P<0.05 was considered to indicate a statistically significant difference.

Results

4-MD suppresses the proliferation, migration and invasion of A549 cells. In the present study, A549 cells were treated with increasing concentrations of 4-MD for 24 h (Fig. 1A). The results demonstrated that 4-MD treatment (≥6.25 μM) significantly reduced cell viability, and the IC_{50} of 4-MD was 83.05 μM (Fig. 1B); therefore, 12.5, 25 and 50 μM 4-MD were used in subsequent experiments, since 4-MD concentrations higher than the IC_{50} may cause cytotoxicity. The experiments were performed at concentrations below IC_{50} to better assess the effect of 4-MD on the cells, which is also the most common criteria for selecting drug concentrations (19). Collectively, the results of cell experiments demonstrated that 4-MD reduced cell viability, colony formation and the number of EDU-positive cells in a concentration-dependent manner, highlighting the anti-proliferative activity of 4-MD in A549 cells (Fig. 1C-E). In addition, the results of the wound healing and Transwell assays revealed that 4-MD significantly suppressed cell migration and invasion in a concentration-dependent manner (Fig. 2A and B). Furthermore, 4-MD markedly upregulated the protein expression levels of E-cadherin, an epithelial cell marker, and downregulated the protein expression levels of N-cadherin and Vimentin, mesenchymal cell markers (Fig. 2C). These

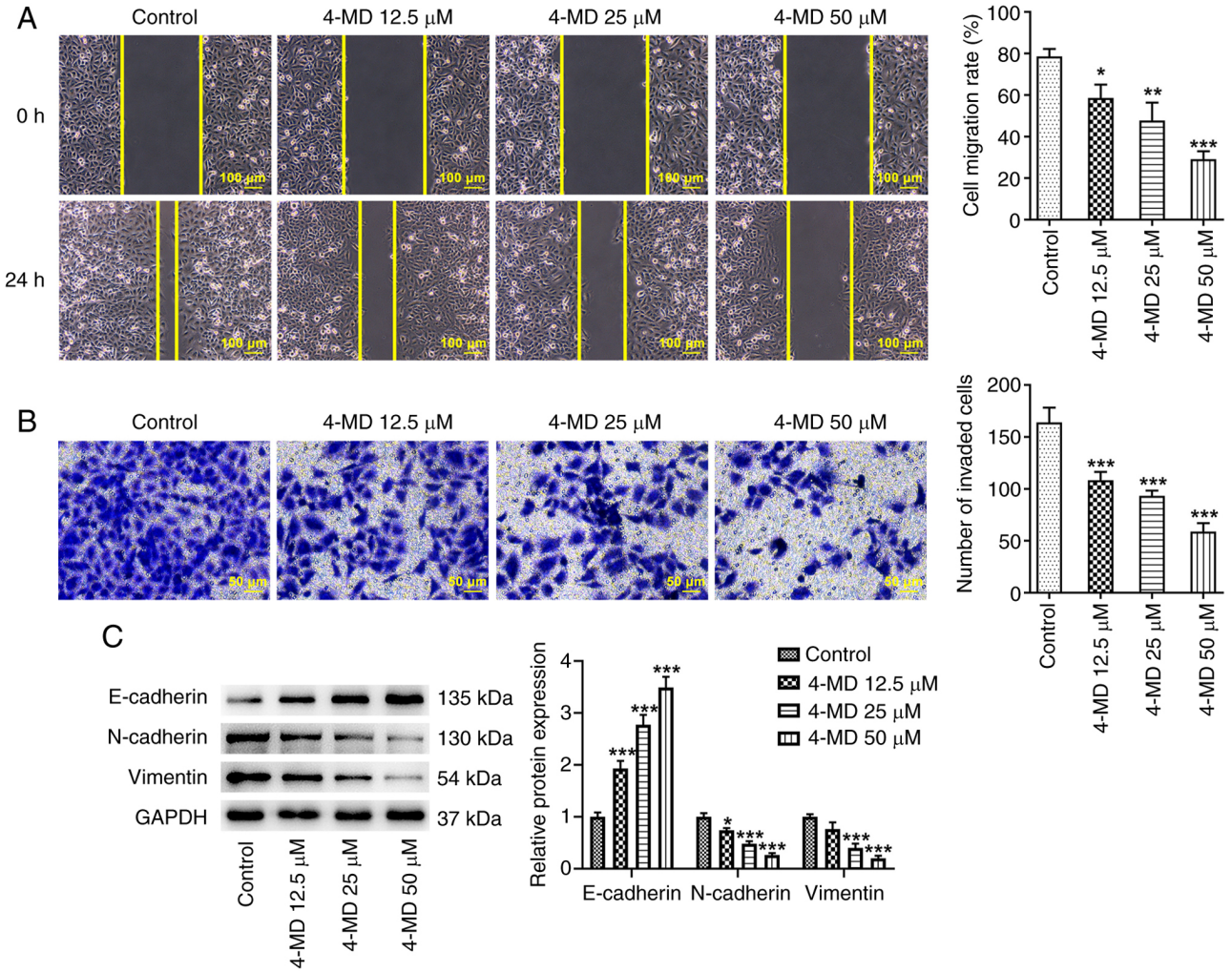

Figure 2. 4-MD suppresses the migration and invasion of A549 cells. (A) A wound healing assay was carried out to assess cell migration. (B) Transwell assay was conducted to assess cell invasion. (C) Epithelial-mesenchymal transition-associated proteins were detected using western blot analysis. *P<0.05, **P<0.01 and ***P<0.001 vs. Control. 4-MD, 4-methoxydalbergione.

results suggested that 4-MD may inhibit epithelial-mesenchymal transition (EMT).

4-MD promotes lipid peroxidation and ferroptosis of A549 cells. The results obtained using transmission electron microscopy demonstrated that A549 cells exhibited mitochondria that were small in size with elevated membrane density following 4-MD treatment, a typical morphological feature of ferroptosis (Fig. 3A). Moreover, TBARS production and levels of lipid ROS were increased following treatment with increasing concentrations of 4-MD, indicating that 4-MD significantly promoted lipid peroxidation (Fig. 3B and C). It was also revealed that A549 cells exhibited an excessive deposition of Fe^{2+} following treatment with 4-MD (Fig. 3D). Notably, ACSL4 is a key step in ferroptosis execution that promotes lipid peroxidation, which is a critical mediator during the modulation of ferroptosis. In the present study, treatment with 4-MD significantly upregulated the protein expression levels of ACSL4 in a concentration-dependent manner (Fig. 3E). Collectively, these results demonstrated that 4-MD induced ferroptosis in A549 cells.

4-MD directly targets DNMT1 to regulate ferroptosis. Further investigations were conducted to elucidate the molecular mechanisms underlying the pro-ferroptosis activity of 4-MD. In the present study, results obtained using TargetNet (http://targetnet.scbdd.com/) revealed that DNMT1 exhibited potential as a target of 4-MD, and further results obtained using molecular docking identified binding sites between DNMT1 and 4-MD (Fig. 4A). The results of a previous study demonstrated that 6-thioguanine, a DNMT1 degrader, inactivated system Xc^{-}, inhibited the production of GSH, reduced GPX4 expression and increased the levels of lipid ROS; thus, promoting Fe^{2+}-dependent ferroptosis. These results suggested that DNMT1 degradation may possess the potential to induce ferroptosis (20). The results of the present study revealed that the protein expression levels of DNMT1, SLC7A11 and GPX4 were significantly reduced in A549 cells following treatment with 4-MD (Fig. 4B). Thus, it was hypothesized that 4-MD may directly bind to DNMT1 for subsequent inhibition, leading to downregulation of SLC7A11 and GPX4, and the induction of ferroptosis.

In the present study, A549 cells were transfected with Oe-DNMT1 to induce DNMT1 overexpression (Fig. 4C and D).

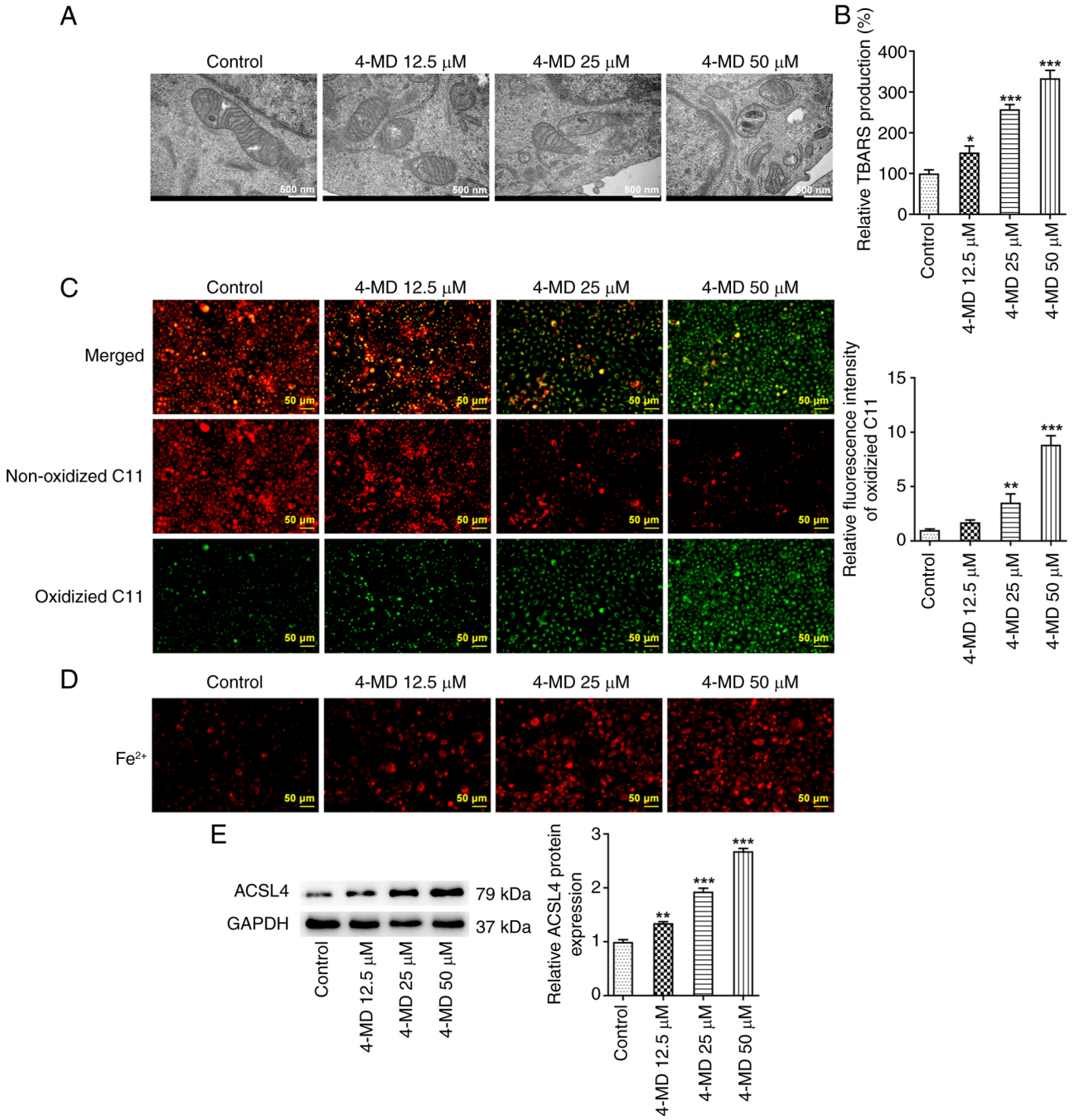

Figure 3. 4-MD promotes lipid peroxidation and ferroptosis of A549 cells. (A) Morphology of A549 cells was observed using transmission electron microscopy. (B) Lipid peroxidation was assessed via TBARS production. (C) Lipid ROS were detected using BODIPY (581/591) C11 staining. (D) Fe^{2+} levels were determined using a FerroOrange probe. (E) Expression of ferroptosis-associated proteins was examined using western blot analysis. *P<0.05, **P<0.01 and ***P<0.001 vs. Control. 4-MD, 4-methoxydalbergione; ACSL4, acyl-CoA synthetase long-chain family 4; ROS, reactive oxygen species; TBARS, thiobarbituric acid reactive substance.

A549 cells with and without Oe-DNMT1 transfection were treated with 50 μM 4-MD. It was revealed that the 4-MD-mediated inhibition of DNMT1, SLC7A11 and GPX4 protein expression levels was partially abolished following DNMT1 overexpression (Fig. 4E). In addition, 4-MD-mediated excessive Fe^{2+} production was markedly reduced following DNMT1 overexpression (Fig. 5A). The results also demonstrated that TBARS production and lipid ROS levels were reduced in the 4-MD + Oe-DNMT1 group, compared with those in the 4-MD + Oe-NC group, highlighting that DNMT1 overexpression inhibited 4-MD-mediated lipid peroxidation in A549 cells (Fig. 5B and C). Moreover, 4-MD-mediated alterations in ACSL4 expression were also reversed following DNMT1 overexpression (Fig. 5D). These findings suggested that 4-MD may promote ferroptosis through regulation of the DNMT1/system Xc^{-}/GPX4 pathway.

DNMT1 overexpression partially abolishes the inhibitory effects of 4-MD on A549 cells. To further determine the regulatory role of the 4-MD/DNMT1 axis in lung cancer, the

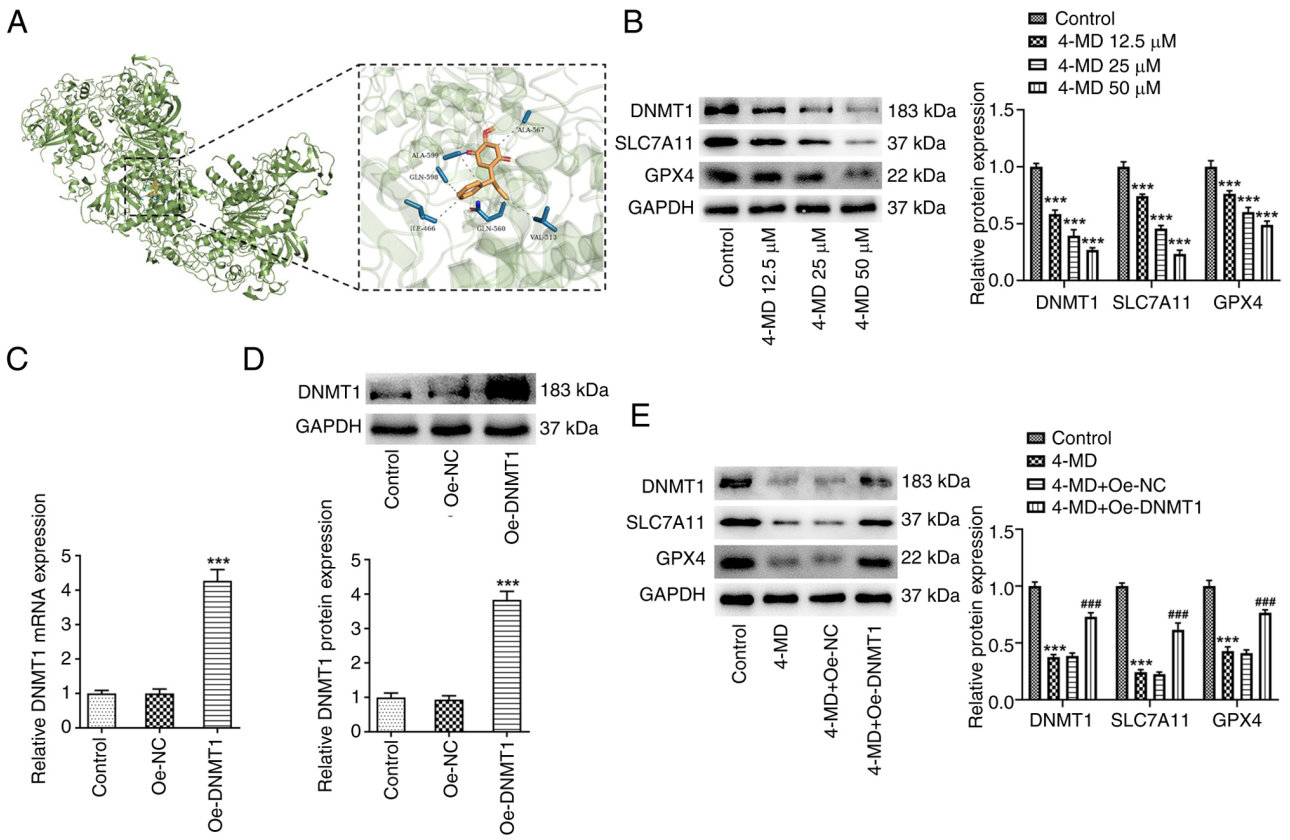

Figure 4. 4-MD directly targets DNMT1 to regulate ferroptosis. (A) Molecular docking between 4-MD and DNMT1. (B) Protein expression of DNMT1, SLC7A11 and GPX4. ***P<0.001 vs. Control. (C) A549 cells were transfected with Oe-NC and Oe-DNMT1, and DNMT1 mRNA expression levels were examined using reverse transcription-quantitative PCR. (D) DNMT1 protein expression levels were examined using western blot analysis. ***P<0.001 vs. Oe-NC. (E) A549 cells and A549 cells transfected with Oe-DNMT1 were treated with 50 μM 4-MD. Protein expression levels of DNMT1, SLC7A11 and GPX4 were detected using western blot analysis. ***P<0.001 vs. Control; ###P<0.001 vs. 4-MD + Oe-NC. 4-MD, 4-methoxydalbergione; DNMT1, DNA methyltransferase 1; GPX4, glutathione peroxidase 4; NC, negative control; Oe, overexpression; SLC7A11, solute carrier family 7 member 11.

malignant behavior of cells was assessed using a rescue assay. As shown in Fig. 6A-C, cell viability, colony number and the number of EDU-positive cells were increased in the 4-MD + Oe-DNMT1 group, compared with those in the 4-MD + Oe-NC group. These results indicated that the 4-MD-mediated effects on A549 cell proliferation were partially abolished following DNMT1 overexpression. Moreover, it was demonstrated that wound healing and cell invasion were increased in the 4-MD + Oe-DNMT1 group, compared with those in the 4-MD + Oe-NC group (Fig. 6D and E). These results indicated that the inhibitory effects of 4-MD on A549 cell migration and invasion were reduced following DNMT1 overexpression. The results of the western blot analysis also demonstrated that the 4-MD-mediated alterations in EMT-associated protein expression levels were partially abolished following DNMT1 overexpression (Fig. 6F).

4-MD reduces tumor growth and promotes ferroptosis in mice. In the present study, animal experiments were carried out to further verify the antitumor activity of 4-MD in lung cancer. Notably, 4-MD significantly reduced tumor size and weight in a concentration-dependent manner, highlighting that 4-MD may suppress tumor growth (Fig. 7A-D). Tumor ulcerations were not observed in the present study. The color of the tumors obtained from the first two animals from the control group in Fig. 7B may be due to bleeding around the tumor, since blood oxidation leads to tumor blackening. Alternatively, the bleeding may be due to local bleeding at the time of A549 cell-inoculation, which was small enough to not be observed at the time of inoculation. Subsequent IHC staining of tumor tissues revealed that DNMT1 and Ki-67 expression levels were reduced following treatment with 4-MD (Fig. 7E and F). Moreover, the results of the Prussian blue staining revealed that iron deposition was present in mice following treatment with 4-MD, and DNMT1, SLC7A11 and GPX4 protein expression levels were markedly reduced (Fig. 7G and H). Collectively, these results demonstrated that 4-MD may promote ferroptosis through the DNMT1/system Xc^-/GPX4 pathway.

Discussion

Lung cancer poses a major threat to human health, with high rates of incidence and mortality (21). According to GLOBOCAN 2020 cancer estimates, lung cancer is the second most frequent malignancy, with an estimated 2.2 million new cancer cases and 1.8 million mortalities worldwide in 2020 (22). Although advances have been made in the treatment of lung cancer, the prognosis of patients remains unsatisfactory, and tumor metastasis and recurrence are key factors in treatment failure (23). Thus, the development of novel therapeutic strategies for lung cancer is required. The results of the present study highlighted that 4-MD may exhibit potential in the treatment of lung cancer, through inhibiting cell proliferation, migration and

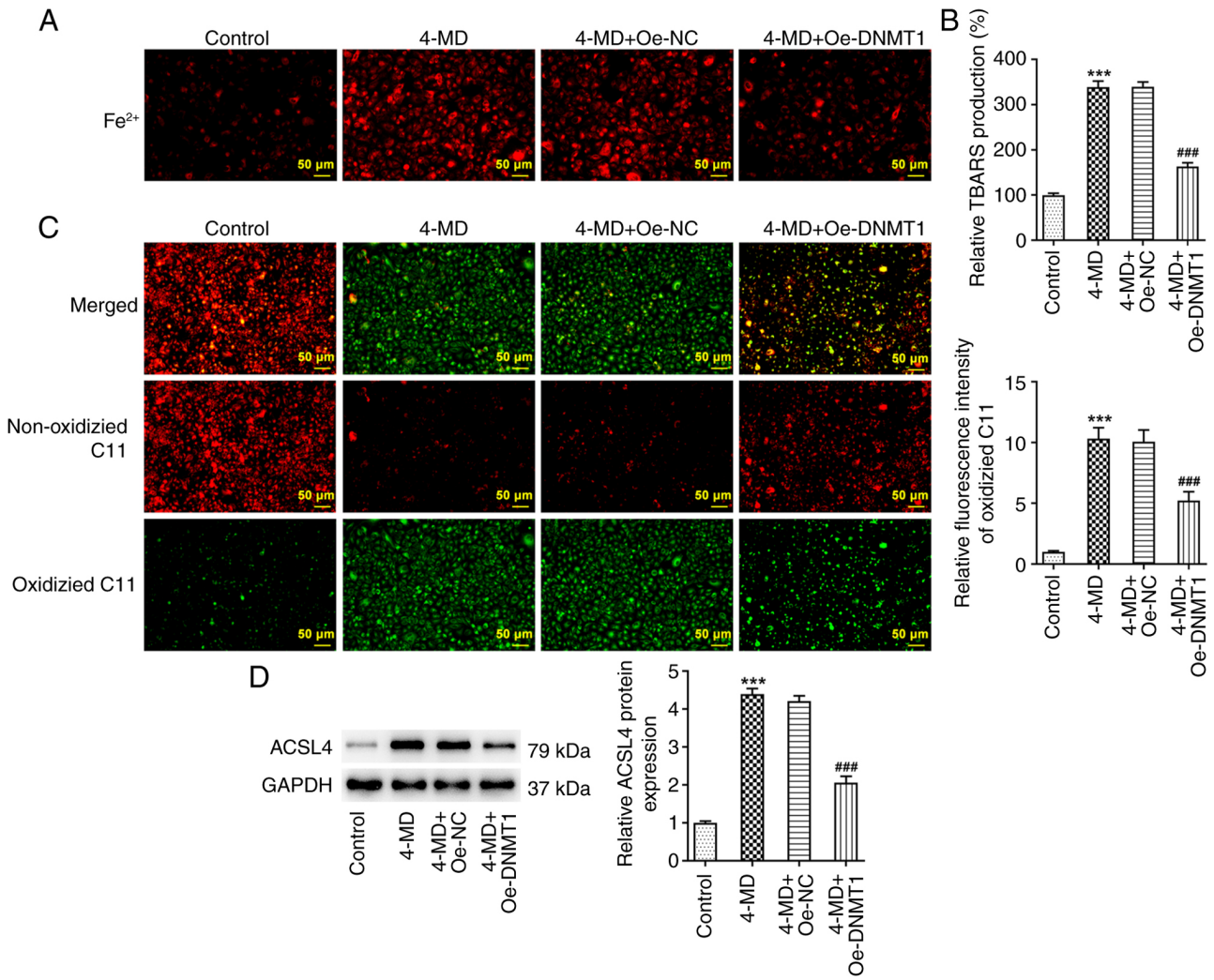

Figure 5. Oe-DNMT1 partially inhibits 4-MD-mediated ferroptosis in A549 cells. (A) Fe^{2+} levels were determined using a FerroOrange probe. (B) Lipid peroxidation was assessed via TBARS production. (C) Lipid ROS levels were detected using BODIPY (581/591) C11 staining. (D) Expression of ferroptosis-associated proteins was determined using western blot analysis. ***P<0.001 vs. Control; $^{###}$P<0.001 vs. 4-MD + Oe-NC. 4-MD, 4-methoxydalbergione; ACSL4, acyl-CoA synthetase long-chain family 4; DNMT1, DNA methyltransferase 1; NC, negative control; Oe, overexpression; ROS, reactive oxygen species; TBARS, thiobarbituric acid reactive substance.

invasion *in vitro,* and limiting tumor growth *in vivo*. Further exploration of the specific molecular mechanisms revealed that 4-MD may target DNMT1 directly, subsequently reducing expression and inducing ferroptosis via the DNMT1/system X_c^-/GPX4 pathway.

Tumor metastasis is a complex biological process involving multiple influencing factors and molecular mechanisms. Notably, EMT is crucial in facilitating the motility and invasion of solid tumor cells, and is the key initial step in cancer cell metastasis (24-26). During EMT, cells presenting with epithelium-associated phenotypes and behaviors undergo a transitional process, leading to the development of mesenchymal phenotypes, and increased migration and invasion. During metastasis, the expression of the epithelial adhesion protein, E-cadherin, is reduced, whereas the expression of mesenchymal markers, including N-cadherin and Vimentin, is increased (21,27). The results of a previous study demonstrated that natural compounds and reagents that exert EMT-suppressive activity may exhibit potential in the treatment of lung cancer (26). The present study demonstrated that E-cadherin expression levels were significantly increased in A549 cells, whereas the expression levels of Vimentin and N-cadherin were markedly decreased following treatment with 4-MD. Thus, 4-MD may exhibit potential in reducing the proliferation and invasion of A549 cells.

Active components of Traditional Chinese Medicine are considered inducers of ferroptosis; thus, exhibiting potential in the treatment of cancer (28). The results of a previous study demonstrated that Sanguinarine, a natural benzophenanthridine alkaloid derived from the root of *Sanguinaria canadensis* Linn., inhibited the growth and metastasis of lung cancer through facilitating GPX4-dependent ferroptosis (29). Shikonin, the major active constituent purified from the roots of *Lithospermum erythrorhizon*, has been shown to significantly inhibit cell proliferation, migration and invasion, and reduce tumor growth in lung cancer through inducing ferroptosis (30). Thus, compounds that target ferroptosis may exhibit potential in the treatment of lung cancer. The results of the present study indicated that 4-MD may significantly induce ferroptosis in lung cancer cells. Notably, multiple

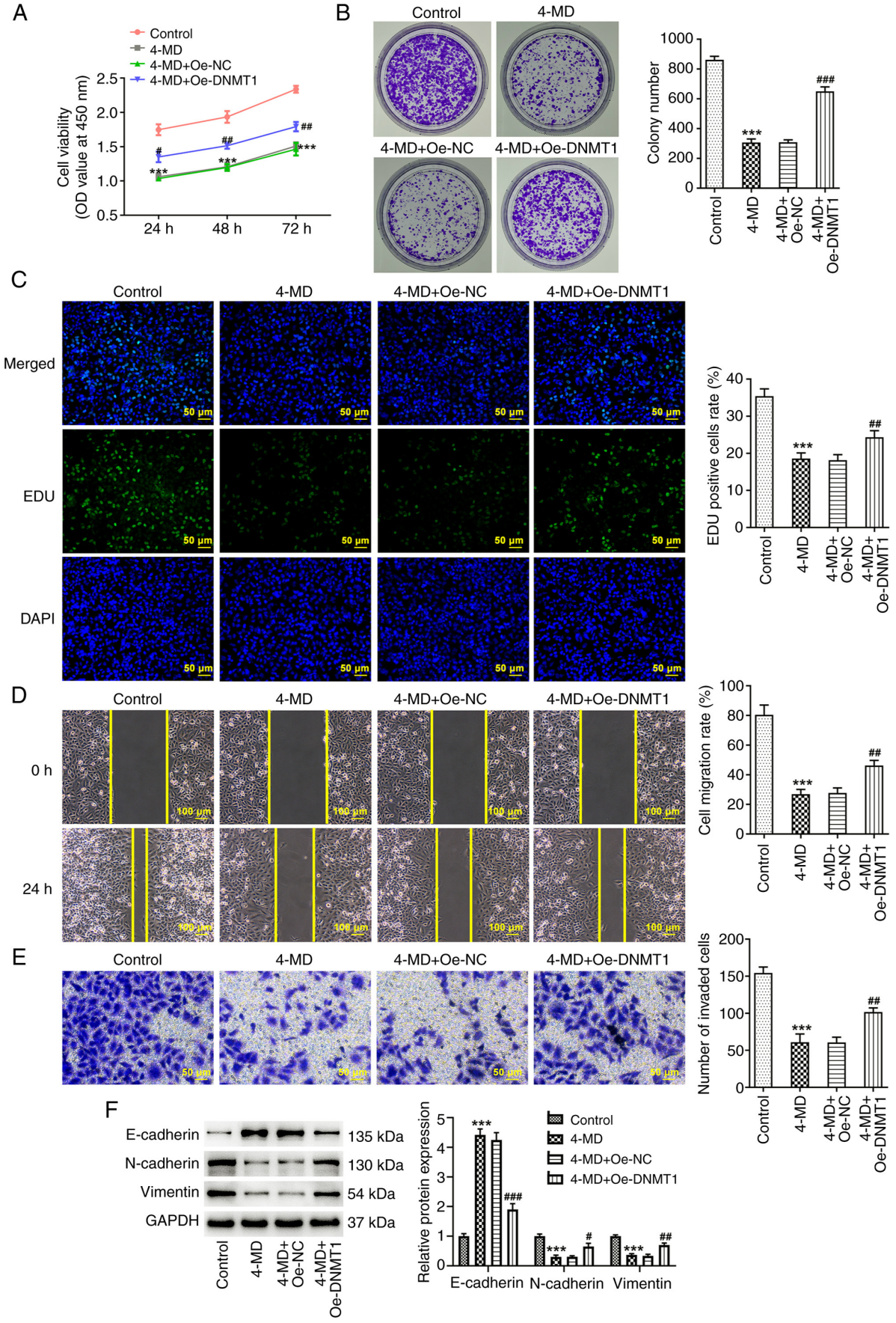

Figure 6. Oe-DNMT1 partially abolishes the inhibitory effects of 4-MD on the malignant behavior of A549 cells. (A) Cell viability was assessed using a CCK-8 assay. (B) Colony formation assay was performed to examine the A549 cell proliferation. (C) EDU staining was performed to assess cell proliferation. (D) A wound healing assay was carried out to assess cell migration. (E) Transwell assay was performed to assess cell invasion. (F) Epithelial-mesenchymal transition-associated proteins were determined using western blot analysis. ***P<0.001 vs. Control; $^{\#}$P<0.05, $^{\#\#}$P<0.01 and $^{\#\#\#}$P<0.001 vs. 4-MD + Oe-NC. 4-MD, 4-methoxydalbergione; DNMT1, DNA methyltransferase 1; NC, negative control; Oe, overexpression.

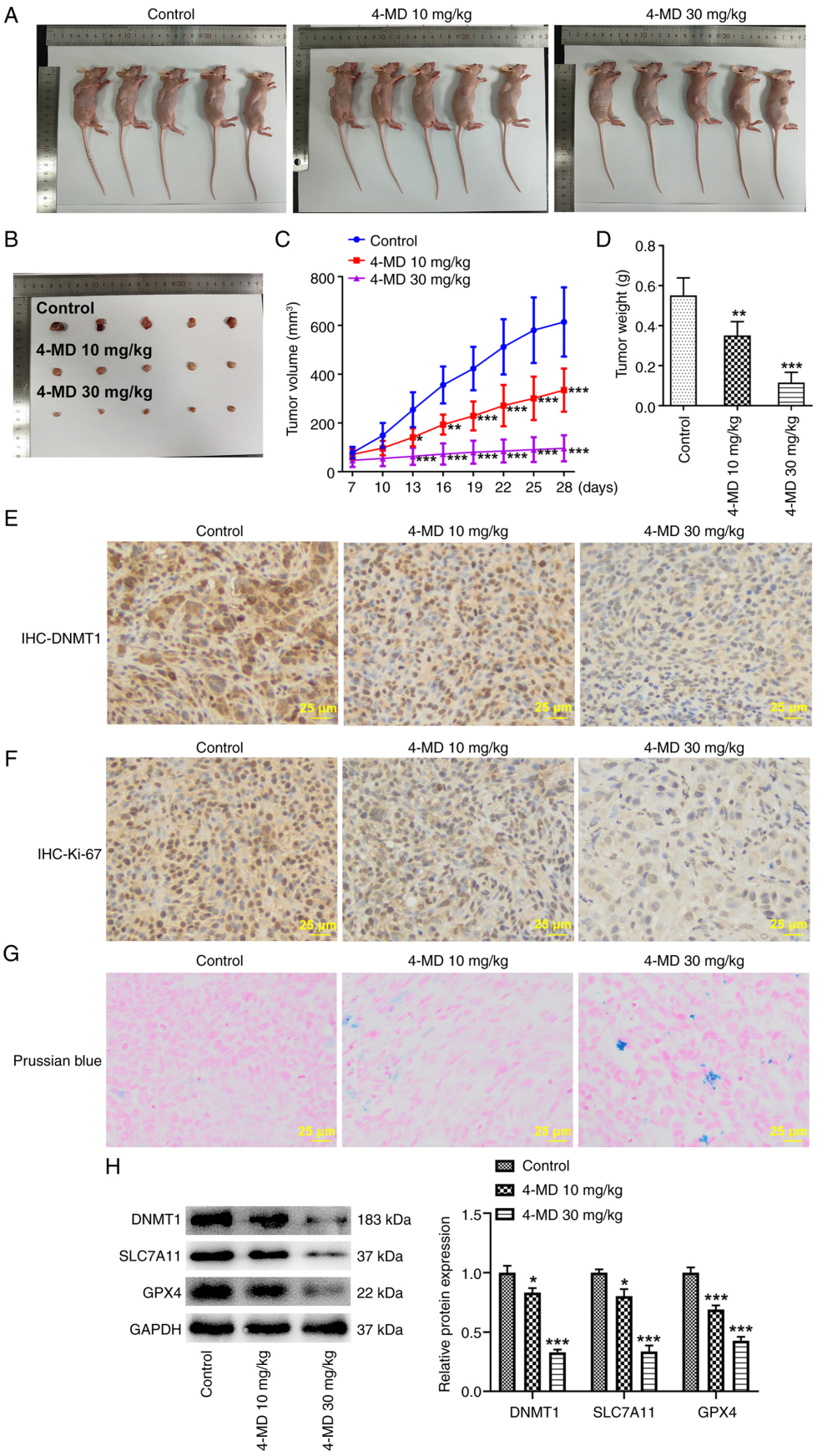

Figure 7. 4-MD inhibits tumor growth and promotes ferroptosis in mice. (A) In total, $4x10^6$ A549 cells were subcutaneously injected into the right flank of each mouse, and mice were intraperitoneally injected with 4-MD (10 or 30 mg/kg) every 3 days for 3 weeks. (B) Images of tumors in nude mice. (C) Tumor volume was measured and calculated every 3 days. (D) Tumor weight. IHC was conducted to detect (E) DNMT1 and (F) Ki-67 expression in tumor tissues of nude mice. (G) Prussian blue staining was used to assess iron deposition. (H) Protein expression levels of DNMT1, SLC7A11 and GPX4 were examined in tumor tissues using western blot analysis. *P<0.05, **P<0.01 and ***P<0.001 vs. Control. 4-MD, 4-methoxydalbergione; DNMT1, DNA methyltransferase 1; GPX4, glutathione peroxidase 4; IHC, immunohistochemistry; SLC7A11, solute carrier family 7 member 11.

factors are involved in the modulation of ferroptosis, including GPX4, SLC7A11 and ACSL4. At present, two mechanisms are considered inducers of ferroptosis; namely, GPX4 inhibition and system Xc^- inhibition (31). The present study revealed that 4-MD may inhibit GPX4 and SLC7A11 expression. Thus, 4-MD may exhibit potential in the treatment of cancer through the induction of ferroptosis.

Drug-target interactions are critical for the development of novel therapeutic strategies; however, identification of potential targets is complex. In the present study, TargetNet (32), an open website for predicting target binding in molecules, was used to predict the potential target of 4-MD. The results obtained using TargetNet and molecular docking demonstrated that 4-MD may directly bind to DNMT1. DNMT1, a maintenance DNA methyltransferase, is upregulated in lung cancer. This protein increases the methylation of tumor suppressor gene promoters to inhibit gene expression, thus facilitating the development of lung cancer (33,34). The results of a previous study revealed that DNMT1 can inhibit ferroptosis through regulating the methylation of ferroptosis-associated genes (35). Moreover, 6-thioguanine, a DNMT1 degrader, has been reported to inactivate system Xc^- and downregulate the expression of GPX4; thus, inducing ferroptosis via the inhibition of DNMT1 (20). These findings suggested that DNMT1 inhibition may exhibit potential in promoting ferroptosis. In the present study, the results of the rescue assay revealed that the anticancer activity and ferroptosis-promoting effects of 4-MD in lung cancer were partially abolished following DNMT1 overexpression. Thus, 4-MD may reduce the progression of lung cancer through the inhibition of DNMT1.

To the best of our knowledge, the present study is the first to demonstrate the anticancer activity of 4-MD in lung cancer. The results of the present study revealed that 4-MD effectively suppressed cell proliferation, migration and invasion, and reduced EMT in A549 cells, and inhibited tumor growth *in vivo*. Mechanistically, 4-MD may directly bind to DNMT1, thus exerting anticancer effects via the inhibition of DNMT1. Moreover, 4-MD may induce ferroptosis in lung cancer cells via the DNMT1/system Xc^-/GPX4 pathway. Therefore, 4-MD may exhibit potential as a novel therapeutic agent in the treatment of lung cancer.

Acknowledgements

Not applicable.

Funding

This study was supported by the National Natural Science Foundation of China (grant no. 81972175).

Availability of data and materials

The data generated in the present study may be requested from the corresponding author.

Authors' contributions

LC designed the study. JF, HL and JL conducted the experiments and analyzed the data. JF and HL drafted the manuscript, and LC critically revised the manuscript. JF and LC confirm the authenticity of all the raw data. All authors read and approved the final version of the manuscript.

Ethics approval and consent to participate

All animal studies were carried out in compliance with the ARRIVE guidelines and were approved by the Animal Ethics Committee of The First Affiliated Hospital of Nanjing Medical University (approval no. IACUC-230814).

Patient consent for publication

Not applicable.

Conflict of interest

The authors declare that they have no competing interests.

References

1. Siegel RL, Miller KD, Wagle NS and Jemal A: Cancer statistics, 2023. CA Cancer J Clin 73: 17-48, 2023.
2. Siegel RL, Miller KD and Jemal A: Cancer statistics, 2019. CA Cancer J Clin 69: 7-34, 2019.
3. Kim N, Kim HK, Lee K, Hong Y, Cho JH, Choi JW, Lee JI, Suh YL, Ku BM, Eum HH, *et al*: Single-cell RNA sequencing demonstrates the molecular and cellular reprogramming of metastatic lung adenocarcinoma. Nat Commun 11: 2285, 2020.
4. Lambert AW, Pattabiraman DR and Weinberg RA: Emerging biological principles of metastasis. Cell 168: 670-691, 2017.
5. Luo H, Vong CT, Chen H, Gao Y, Lyu P, Qiu L, Zhao M, Liu Q, Cheng Z, Zou J, *et al*: Naturally occurring anti-cancer compounds: Shining from Chinese herbal medicine. Chin Med 14: 48, 2019.
6. Chan SC, Chang YS, Wang JP, Chen SC and Kuo SC: Three new flavonoids and antiallergic, anti-inflammatory constituents from the heartwood of Dalbergia odorifera. Planta Med 64: 153-158, 1998.
7. Kim DC, Lee DS, Ko W, Kim KW, Kim HJ, Yoon CS, Oh H and Kim YC: Heme Oxygenase-1-Inducing Activity of 4-Methoxydalbergione and 4'-Hydroxy-4-methoxydalbergione from Dalbergia odorifera and Their Anti-inflammatory and Cytoprotective Effects in Murine Hippocampal and BV2 microglial cell line and primary rat microglial cells. Neurotox Res 33: 337-352, 2018.
8. Du H, Tao T, Xu S, Xu C, Li S, Su Q, Yan J, Liu B and Li R: 4-Methoxydalbergione Inhibits Bladder Cancer Cell Growth via Inducing Autophagy and Inhibiting Akt/ERK Signaling Pathway. Front Mol Biosci 8: 789658, 2022.
9. Zeng L, Qin Y, Lu X, Fang X, Huang J, Yu C and Feng ZB: 4-Methoxydalbergione Elicits Anticancer Effects by Upregulation of GADD45G in Human Liver Cancer Cells. J Healthc Eng 2023: 6710880, 2023.
10. Li M, Xiao Y, Liu P, Wei L, Zhang T, Xiang Z, Liu X, Zhang K, Zhong Q and Chen F: 4-Methoxydalbergione inhibits esophageal carcinoma cell proliferation and migration by inactivating NF-κB. Oncol Rep 49: 42, 2023.
11. Li R, Xu CQ, Shen JX, Ren QY, Chen DL, Lin MJ, Huang RN, Li CH, Zhong RT, Luo ZH, *et al*: 4-Methoxydalbergione is a potent inhibitor of human astroglioma U87 cells in vitro and in vivo. Acta Pharmacol Sin 42: 1507-1515, 2021.
12. Park KR, Yun HM, Quang TH, Oh H, Lee DS, Auh QS and Kim EC: 4-Methoxydalbergione suppresses growth and induces apoptosis in human osteosarcoma cells in vitro and in vivo xenograft model through down-regulation of the JAK2/STAT3 pathway. Oncotarget 7: 6960-6971, 2016.
13. Yan HF, Zou T, Tuo QZ, Xu S, Li H, Belaidi AA and Lei P: Ferroptosis: Mechanisms and links with diseases. Signal Transduct Target Ther 6: 49, 2021.
14. Hassannia B, Vandenabeele P and Vanden Berghe T: Targeting ferroptosis to iron out cancer. Cancer Cell 35: 830-849, 2019.

15. Liang C, Zhang X, Yang M and Dong X: Recent progress in ferroptosis inducers for cancer therapy. Adv Mater 31: e1904197, 2019.
16. Livak KJ and Schmittgen TD: Analysis of relative gene expression data using real-time quantitative PCR and the 2(-Delta Delta C(T)) Method. Methods 25: 402-408, 2001.
17. Percie du Sert N, Hurst V, Ahluwalia A, Alam S, Avey MT, Baker M, Browne WJ, Clark A, Cuthill IC, Dirnagl U, *et al*: The ARRIVE guidelines 2.0: Updated guidelines for reporting animal research. PLoS Biol 18: e3000410, 2020.
18. Pritt SL and Smith TM: Institutional animal care and use committee postapproval monitoring programs: A proposed comprehensive classification scheme. J Am Assoc Lab Anim Sci 59: 127-131, 2020.
19. Zhang X, Wang R, Piotrowski M, Zhang H and Leach KL: Intracellular concentrations determine the cytotoxicity of adefovir, cidofovir and tenofovir. Toxicol In Vitro 29: 251-258, 2015.
20. Zhang J, Gao M, Niu Y and Sun J: From DNMT1 degrader to ferroptosis promoter: Drug repositioning of 6-Thioguanine as a ferroptosis inducer in gastric cancer. Biochem Biophys Res Commun 603: 75-81, 2022.
21. Zeng J, Li X, Liang L, Duan H, Xie S and Wang C: Phosphorylation of CAP1 regulates lung cancer proliferation, migration, and invasion. J Cancer Res Clin Oncol 148: 137-153, 2022.
22. Sung H, Ferlay J, Siegel RL, Laversanne M, Soerjomataram I, Jemal A and Bray F: Global Cancer Statistics 2020: GLOBOCAN estimates of incidence and mortality worldwide for 36 cancers in 185 countries. CA Cancer J Clin 71: 209-249, 2021.
23. Muthusamy B, Patil PD and Pennell NA: Perioperative systemic therapy for resectable non-small cell lung cancer. J Natl Compr Canc Netw 20: 953-961, 2022.
24. Xie S, Wu Z, Qi Y, Wu B and Zhu X: The metastasizing mechanisms of lung cancer: Recent advances and therapeutic challenges. Biomed Pharmacother 138: 111450, 2021.
25. Bakir B, Chiarella AM, Pitarresi JR and Rustgi AK: EMT, MET, plasticity, and tumor metastasis. Trends Cell Biol 30: 764-776, 2020.
26. Chanvorachote P, Petsri K and Thongsom S: Epithelial to mesenchymal transition in lung cancer: Potential EMT-Targeting natural product-derived compounds. Anticancer Res 42: 4237-4246, 2022.
27. Menju T and Date H: Lung cancer and epithelial-mesenchymal transition. Gen Thorac Cardiovasc Surg 69: 781-789, 2021.
28. Ye J, Zhang R, Wu F, Zhai L, Wang K, Xiao M, Xie T and Sui X: Non-apoptotic cell death in malignant tumor cells and natural compounds. Cancer Lett 420: 210-227, 2018.
29. Xu R, Wu J, Luo Y, Wang Y, Tian J, Teng W, Zhang B, Fang Z and Li Y: Sanguinarine represses the growth and metastasis of non-small cell lung cancer by facilitating ferroptosis. Curr Pharm Des 28: 760-768, 2022.
30. Qian X, Zhu L, Xu M, Liu H, Yu X, Shao Q and Qin J: Shikonin suppresses small cell lung cancer growth via inducing ATF3-mediated ferroptosis to promote ROS accumulation. Chem Biol Interact 382: 110588, 2023.
31. Yang WS and Stockwell BR: Ferroptosis: Death by lipid peroxidation. Trends Cell Biol 26: 165-176, 2016.
32. Yao ZJ, Dong J, Che YJ, Zhu MF, Wen M, Wang NN, Wang S, Lu AP and Cao DS: TargetNet: A web service for predicting potential drug-target interaction profiling via multi-target SAR models. J Comput Aided Mol Des 30: 413-424, 2016.
33. Wu XY, Chen HC, Li WW, Yan JD and Lv RY: DNMT1 promotes cell proliferation via methylating hMLH1 and hMSH2 promoters in EGFR-mutated non-small cell lung cancer. J Biochem 168: 151-157, 2020.
34. Ma F, Lei YY, Ding MG, Luo LH, Xie YC and Liu XL: LncRNA NEAT1 Interacted With DNMT1 to regulate malignant phenotype of cancer cell and cytotoxic T Cell Infiltration via Epigenetic Inhibition of p53, cGAS, and STING in Lung Cancer. Front Genet 11: 250, 2020.
35. Zou P, Chen Z, He Q and Zhuo Y: Polyphyllin I induces ferroptosis in castration-resistant prostate cancer cells through the ERK/DNMT1/ACSL4 axis. Prostate 84: 64-73, 2024.